UNIVERSITÀ DI PARMA
ARCHIVIO DELLA RICERCA

University of Parma Research Repository

Macroalgae to Nanoparticles: study of Ulva lactuca L. role in biosynthesis of gold and silver nanoparticles and of their cytotoxicity on colon cancer cell lines

note finali coverpage

(Article begins on next page)

21 February 2025

Accepted Manuscript

Macroalgae to nanoparticles: Study of Ulva lactuca L. role in biosynthesis of gold and silver nanoparticles and of their cytotoxicity on colon cancer cell lines

Noelia González-Ballesteros, M. Carmen Rodríguez-Argüelles, Sonia Prado-López, Mariano Lastra, Maria Grimaldi, Antonella Cavazza, Lucia Nasi, Giancarlo Salviati, Franca Bigi

Macroalgae to Nanoparticles: study of *Ulva lactuca* L. role in biosynthesis of gold and silver nanoparticles and of their cytotoxicity on colon cancer cell lines

Noelia González-Ballesteros[a], M. Carmen Rodríguez-Argüelles[a]*, Sonia Prado-López[b], Mariano *Lastra*[c], *Maria Grimaldi*[d], *Antonella Cavazza*[d], *Lucia Nasi*[e], *Giancarlo Salviati*[e] *and Franca Bigi*[d]

[a]*Departamento de Química Inorgánica. CINBIO. Universidade de Vigo, 36310 Vigo, Spain.*

[b]*Departamento de Genética, Bioquímica e Inmunología. Universidade de Vigo, 36310 Vigo, Spain.*

[c]*Estación de Ciencias Marinas de Toralla (ECIMAT), Universidade de Vigo, 36331 Vigo, Spain.*

[d]*Dipartimento Scienze Chimiche, della Vita e della Sostenibilità Ambientale. Università di Parma, 43124 Parma (Italy)*

[e]*CNR-IMEM. 43124 Parma (Italy)*

ABSTRACT

Marine bio-resources are being widely studied as an invaluable source of compounds with therapeutic applicability. In particular, macroalgae contain an extended variety of bioactive compounds with different structures and promising biological applications. In this work, *Ulva lactuca* L. (hereafter UL) was utilyzed for the synthesis of gold and silver nanoparticles. Full characterization by UV-Vis spectroscopy, TEM, HRTEM and STEM miscroscopies, Z Potential and FTIR spectroscopy was performed. The first time in the scientific literature, the composition of carbohydrates of UL extract and their changes observed after nanoparticles synthesis were explored in order to investigate their possible role in the biosynthetic process. The reducing power, total phenolic content and DPPH scavenging activity of UL extract, Au@UL and Ag@UL nanoparticles were determined. The effects of UL extract, Au@UL and Ag@UL were tested *in vitro* on the colon cancer cell lines HT-29 and Caco-2, on normal primary neonatal dermal fibroblast cell line PCS-201-010, as well as on normal colon cell line CCD-112CoN. Lastly, the apoptotic activity and cellular uptake evaluation was determined for Au@UL and Ag@UL.

Keywords: *Ulva lactuca,* AuNP, AgNP, Caco-2, HT-29.

1. Introduction

Natural resources have been an invaluable source of new compounds with therapeutic utility.[1] Among these, marine resources are gaining an increasing attention. Compounds from marine bio-resources, including animals, seaweeds, bacteria and fungi, are being widely investigated and used due to their potentially useful biological activities. In particular, macroalgae contain a wide variety of bioactive compounds with different structures and promising biological applications.[2] The major

components in macroalgae are polysaccharides, which can range from 4 to 76% of algal dry weight. It has been demonstrated that macroalgae derived polysaccharides have a large array of biotechnological and biomedical applications, including cancer therapy, immune regulation and antiviral activity.[2,3]

Recently, algae have been labeled as "nanofactories", due to their potential use in nanomaterial biosynthesis. The biological synthesis of metal nanoparticles meets the criteria of green chemistry for being one of the most environmentally friendly methods. The major effect of this green synthesis is the lack of toxic solvents and reagents, preventing by-products and waste generation during metal nanoparticle synthesis. It also promotes the use of renewable natural resources.[4] However, the methods for achieving the desirable size, shape, stability, and controlled crystal growth structure request further investigation.[5]

In the framework of our research project addressed to test potential uses of macroalgaes as reducing and stabilizing agents for the green synthesis of nanomaterials with application in nanomedicine,[6] we have focused our attention on *Ulva lactuca* L. (UL), a common species of green algae in the division Chlorophyta. It is a cosmopolitan and opportunistic blade shape macroalgae worldwide distributed that proliferates in euthrophic conditions. A large amoung of UL is washed ashore on the beaches every year; decomposition of these tidal deposits produce methane, hydrogen sulphide and other gases that are not environmental friendly.[3] Due to its abundance and the ecological problems that create, UL has been studied in the latest years UL to optimise its aplications in pharmacology, cosmetic and food industry. The chemical composition of UL is complex, and may be affected by seasonality, origin, growth conditions, etc. Different studies reported on the isolation, purification and chemical structure of sulphated polysaccharide from UL, known as Ulvan.[3] Furthermore, recent studies on UL have been focused on its application in tissues engineering,[2,7] drug delivery[7] and antitumoral activity has been also studied.[8,9] In the last years, there has been increasing number of studies reporting on the application of UL in the synthesis of silver nanoparticles led by UL extract.[10-13]

Here, we propose a critical revision of the application of UL in the synthesis of silver nanoparticles and, to the best of our knowledge, we also provide the first evidence on the biosynthesis of gold nanoparticles led by UL. In addition, we report on the composition of UL and on its changes observed during the synthesis of the Au and Ag nanoparticles. Since both UL and gold nanoparticles have been reported to hold anti-tumour activity by its own, [14] we expect to obtain an improved synergic effect in our Au@UL system. In this respect, the in vitro anti tumor activity on colon cancer cell lines is also examined.

2. Experimental Section

All reagents were utilized without further purification in the assays. Milli-Q water was used at any

step throughout the experiments. All glassware was clean as previously described[6].

2.1. Preparation and characterization of UL extract

Thalli of live bunches of UL were collected at the lower intertidal rocky shore in the NW coast of Spain (42º 12' 2.9'' N; 8º 47' 6.2'' W). Samples were either immediately processed or frozen at -24 ºC until treatment. Firstly, the seaweeds were thoroughly rinsed with Milli-Q water to remove seawater, sand and associated biota. Next, fronds were extended on blotting paper to remove excess of water prior to processing. Fragments of seaweeds were cut into fine pieces and placed in a two-necked round-bottomed flask connected to a refrigerant. Milli-Q water was added in a proportion of 1 g/mL and the mixture was then boiled at reflux for 15 minutes. Once the colour changed to greenish, the flask was moved to an ice bath to finish with the extraction. The extract was thus centrifuged in a Beckman coulter Microfuge 16 at 4500 rpm for 10 minutes and the supernatant was filtered. Part of the extract obtained was stored at 4 ºC and the remnant was frozen at -4 ºC, until further treatment.

2.2. Analysis of carbohydrates

The analysis of free carbohydrate fraction was performed on the extracts before and after nanoparticles formation. A centrifugation step was conducted prior to the analysis to remove nanoparticles. High performance anionic exchange chromatography coupled to pulsed amperometric detection (HPAEC-PAD, from Dionex) was used, equipped with a Dionex CarboPac^{TM} SA10 column (4 x 250 mm). Elution was achieved by an opportune gradient system by combining 600 mM NaOH, water and 500 mM sodium acetate at flow of 1.0 mL/min. Standards of carbohydrates (glycerol, eritritol, xylitol, mannitol, ramnose, glucose, mannose, xylose) were purchased from Sigma Aldrich.

2.3. Preparation of Au@UL and Ag@UL

Different reaction conditions were tested to optimize the synthesis of both types of nanoparticles. In all cases the reaction outcome was monitored by UV-Vis spectroscopy. The best reaction conditions are briefly described below.

In the case of Au@UL the best results were obtained for a concentration of extract of 1 g/mL and a final gold concentration of 0.4 mM. This solution was kept at room temperature while stirring for 24 hours. pH measurements were performed prior and after the synthesis, obtaining values of pH=6.37 for the UL extract and 4.28 in the case of Au@UL. The reaction was time scalled in order to understand its evolution in detail. UV-Vis spectra were recorded at the maximum wavelength every 10 minutes for 800 minutes.

Regarding Ag@UL, the best reaction conditions were at an extract concentration of 0.5 g/mL and final silver concentration of 0.17 mM. The extract was heated at reflux, then $AgNO_3$ 0.005 M was added. A color change to yellow was observed after 8 hours of reaction. pH measurements showed a sligh variation from 6.76 to 6.12 after Ag@UL synthesis.

The prepared nanoparticles were fully characterized and employed for the determination of the

cytotoxic activity without further purification.

2.4. Characterization of Au@UL and Ag@UL

UV-Vis spectra were recorded at room temperature on a Jasco Spectrometer V-670. Gold concentration was determined by using a Perkin Elmer Optima-4300 DV ICP-OES with Indium as internal standard.

Zeta potential of Au@UL and Ag@UL was obtained through electrophoretic mobility by taking the average of four measurements at the stationary level using a ZetasizerNano S (Malvern Instruments, Malvern U.K.) equipped with 4 mW He−Ne laser, operating at a wavelength of 633 nm.

Jasco FT/IR-6100 spectrophotometer was used to identify the possible biomolecules at a resolution of 4 cm^{-1} in the range of 4000-400 cm^{-1}. UL extract, Ag@UL and Au@UL were placed in an oven at 80 ºC until dry. The dried materials were ground to fine powder and used to record the spectra employing KBr pellet technique. The FTIR spectra of Ulvan from *Ulva armoricana* (Carbosynth) was recorded for comparative purpose.

Transmission electron microscopy (TEM) and scanning transmission electron microscopy (STEM) samples were prepared by dropping the nanoparticles dispersion directly onto a holey carbon film supported on a copper grid. In order to obtain a better quality in the images it was necessary to centrifuge the samples at 10000 rpm for 10 minutes to eliminate part of the extract. TEM, high resolution transmission microscopy (HRTEM) and STEM images were acquired with a JEOL JEM2010F field emission gun TEM, operated at 200 kV. Electron energy loss spectroscopy (EELS) measurements were performed in STEM mode using a Gatan Quantum EELS GIF, with a collection semi-angle of β=16.75 mrad; the energy resolution was ~1.75 eV (FWHM of the zero-loss peak). To avoid the contribution of the carbon film, EELS spectra were measured in areas of the sample positioned upon a hole. Coupling between the STEM unit and the EDS detector (Oxford Inca Energy 200) was used to obtain elemental maps. Data collection and analysis were carried out using Digital Micrograph software by Gatan.

2.5. In vitro antioxidant activity

The reducing power and the content of phenols of the UL extract, Au@UL and Ag@UL were measured following our modified version of the Oyaizu and Folin-Ciocalteu methods, and the results were expressed as mean ± standard deviation.[6] The free radical scavenging activity of the extract on 1, 1-diphenyl-2-picryl-hydrazyl (DPPH) was evaluated following our modified method.[15] The effective concentration required to decrease the initial DPPH concentration by 50% (EC50) was calculated. All trials were three times replicated.

2.6. In vitro cell cytotoxicity assay

The colorectal cancer cell lines Caco-2 and HT-29 were purchased from the American Type Culture Collection. A normal primary neonatal dermal fibroblast cell line PCS-201-010 and a normal

colon cell line CCD-112CoN were used as control of the effect on healthy cells. Both cell cultures were done following the ATCC recommendations. The cells were cultured as previously mentioned. [6]

The cells were treated during 48 hours with UL extract alone at doses of 1, 0.5, 0.25 and 0.125 g/mL, Au@UL at doses (200, 100, 50, 25, 12.5μM [Au]) and Ag@UL (170, 85, 42.5, 21.25, 10.63μM [Ag]).

The cytotoxicity expressed as cell viability (%) was determined by the Vybrant MTT Proliferation assay Kit from Molecular Probes. Dose response curves were built and IC50 values were then calculated with the GraphPad Prims 6 software. The experiment was done 6 times and results are expressed as mean ± standard error.

2.7. In vitro Apoptosis Assay

Apoptosis assay was preformed employing the Annexin V-FIT kit from (Miltenyi Biotec) following the provider recommendations. Cellular lines HT-29, Caco-2, PCS-201-010 and CCD-112CoN at passages between 2 and 5 were cultured in 35 mm cell culture Dishes from CORNING at density 5 x 10^4 during 24 hours. After that, Au@UL and Ag@UL compounds were added to the cultures. The experiment was repeated 3 times following the same protocol. Graphs and statistic analysis consisting of One Way Anova followed by a Tukey´s multiple comparison tests were done with the software GraphPad Prism 6.

2.8. Flow cytometry

The CRC and the normal cell lines were incubated during 12 hours with Au@UL and Ag@UL at concentration 100 μM and taken to the FACS Aria III for further analysis. Untreated cells were employed as control. Cellular uptake of the nanocompounds was quatify following Zuker protocol with some modifications.[16] The experiment was three times replicated.

3. Results and Discussion

3.1. UL Extract

In this study, an aqueous extract of *Ulva lactuca* was obtained. Different extraction conditions were performed using fresh and frozen seaweed biomass; the best conditions for the biosynthesis of the nanoparticles are reported in the experimental section. No differences in efficiency were observed in the biosynthesis of nanoparticles when using fresh or frozen UL.

3.2. Carbohydrate analysis

The analysis of the free sugars profile of the UL extract showed a complex chromatogram characterized by the presence of several peaks belonging to different classes of compounds: alditols, eluted in the first part of the trace (from 2 to 4 minutes), then mono and disaccharides (4-9 minutes), followed by oligosaccharides (from 9 minutes onwards). The identity of the main peaks was obtained

by comparing their retention times with those recorded from standards, and confirmed by spiking the extracts with a small amount of the known compound. Traces of glycerol, mannitol, ramnose, xylose and glucose was confirmed. The monosaccharides composition of the extract was in agreement with literature data, although most of the previous studies were related to hydrolysed extracts.[3] It is worthmentioning that the presence of some alditols (such as glycerol and mannitol), has been never reported before.

After nanoparticles formation, the analysis of the entire carbohydrate profile in the extracts obtained evidenced a number of differences, both from a qualitative and a quantitative point of view (Figure 1). No conspicuous differences were observed between Au@UL and Ag@UL patterns. Many differences in the intensity of peaks belonging to all types of carbohydrates appeared in Au@UL when compared with UL extract. In particular, peaks related to alditols, eluted in the first four minutes, were characterised by a significantly higher relative intensity (as evidenced in the insert of Figure 1). Afterwards, some peaks in monosaccharides and oligosaccharides area appeared with different intensity.

The obtained results provide new information about the possible role of sugars in nanoparticles formation. The involvement of polysaccharides has already been assumed by previous studies, showing the ability of the carbohydrates to interact with metallic ions through noncovalent bonding.[17] That result implies to postulate the occurrence of a redox reaction between the polysaccharide hydroxylic groups and the metal ions.[18] Moreover, the observed increase in alditols (sugars alcohols) suggested that some sugars may be even reduced during nanoparticles biosynthesis. Besides, increses in alditols and monosaccharides might be linked to a possible hydrolytic mechanism of larger molecules.
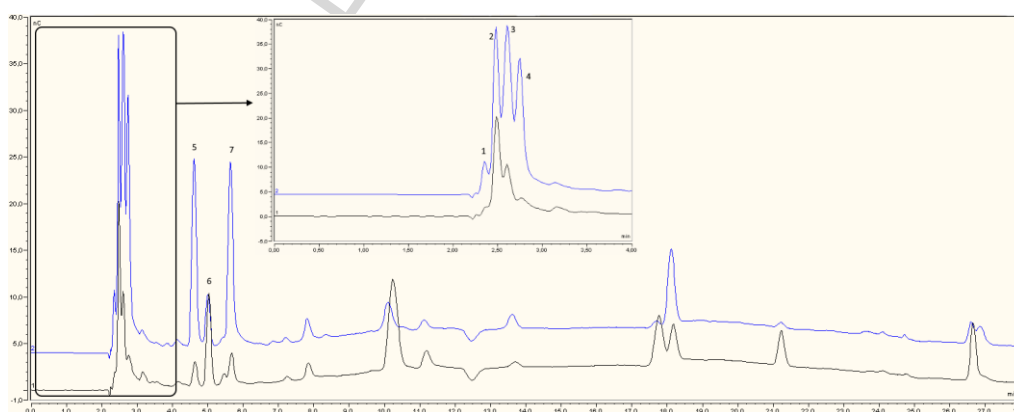
Figure 1. Comparison between the carbohydrate profile of UL extract (below) and the extract obtained after Au@UL formation (above). Insert: expansion of the first part of the chromatogram. Peak identification: 1. and 3. Alditols; 2. Glycerol; 4. Mannitol; 5. Rhamnose; 6. Glucose; 7. Xilose.

3.3. *Synthesis and characterization of Au@UL and Ag@UL*

Aqueous extract of UL was used to reduce of Au(III) to Au(0), and Ag(I) to Ag(0). To attain a narrow size distribution, the optimal reaction conditions were found out after several trials using different experimental conditions, such as seaweed extract concentration, gold or silver concentration, temperature and time. The results on the best conditions are reported in the experimental section. Upon addition of $HAuCl_4$ to the UL extract, the color of the reaction mixture changed from pale yellow to pink within a few hours. UV-Vis spectroscopic analysis of the synthesized Au@UL after 24 hours displayed an intense surface plasmon resonance peak at 529 nm, compared with that of the extract before the reaction (Figure 2A). In order to analyze the reaction process in detail, UV-Vis spectra at the maximum of absorbance wavelength was recorded every 10 minutes, as shown in Figure 2B. The reaction might be divided in three steps. The first one, between 0 and 200 min, was due to the reaction activation. The second one started at 200 min and matched with the beginning of colour change probably attributable to nucleation process. Lastly, the absorbance increased slowly and no variation in color was detected from 500 minutes onwards.

In the case of silver nanoparticles, several assays were conducted until achieving the best reaction conditions for the synthesis of Ag@UL with narrow size distribution. In contrast to some recent reports from literature,[12,19] no color change due to NP formation was observed at room temperature until few days after the starting reaction. Moreover, the particles obtained presented a complex mixture of sizes and shapes. When heating at 100 ºC the reaction is faster and NPs with more homogenous size and shape distribution were obtained. Regarding the optimal concentration, different extract-to-silver ratios were tested, obtaining 0.17 mM as the optimal concentration of Ag. At higher concentration, it was observed that the nanoparticles aggregated and precipitated. The study of the UV-Vis spectra of Ag@UL after 8 hours showed an intense band at 423 nm when compared with the extract before the synthesis (Figure 2A). As previously mentioned, some authors reported on the synthesis of silver nanoparticles with different reaction conditions, thus presenting differences in the wavelength of the SPR band, compared to those obtained in our study. For instance, Devi and Bhimba, Kumar *et al.* and Raja *et al.* reported the SPR band at around 430 nm.[12,13,20] On the other hand, we obtained the same wavelength in the SPR band as reported by Sangeetha and Saravanan.[19] These distinct wavelengths could be due to the differences in the nanoparticles size or to differences in the capping agents of the extracts. The variability in the size distribution obtained will be discussed in the Electron microscopy section.

The stability of the nanoparticles synthetized was measured through the Z Potential analyses. Values of -27.8 ± 0.6 mV and -16.0±0.4 mV were obtained for Au@UL and Ag@UL respectively, which means that Au@UL and Ag@UL form a stable colloidal suspension with the particles that carry a negative electrostatic surface charge.[21] Also, we want to highlight that only one of the

previous papers on silver nanoparticles synthesized by UL reports on Z Potential results; Kumar *et al.* obtained a negative Z potential of -34 mV, what is below values obtained in our study.[12]
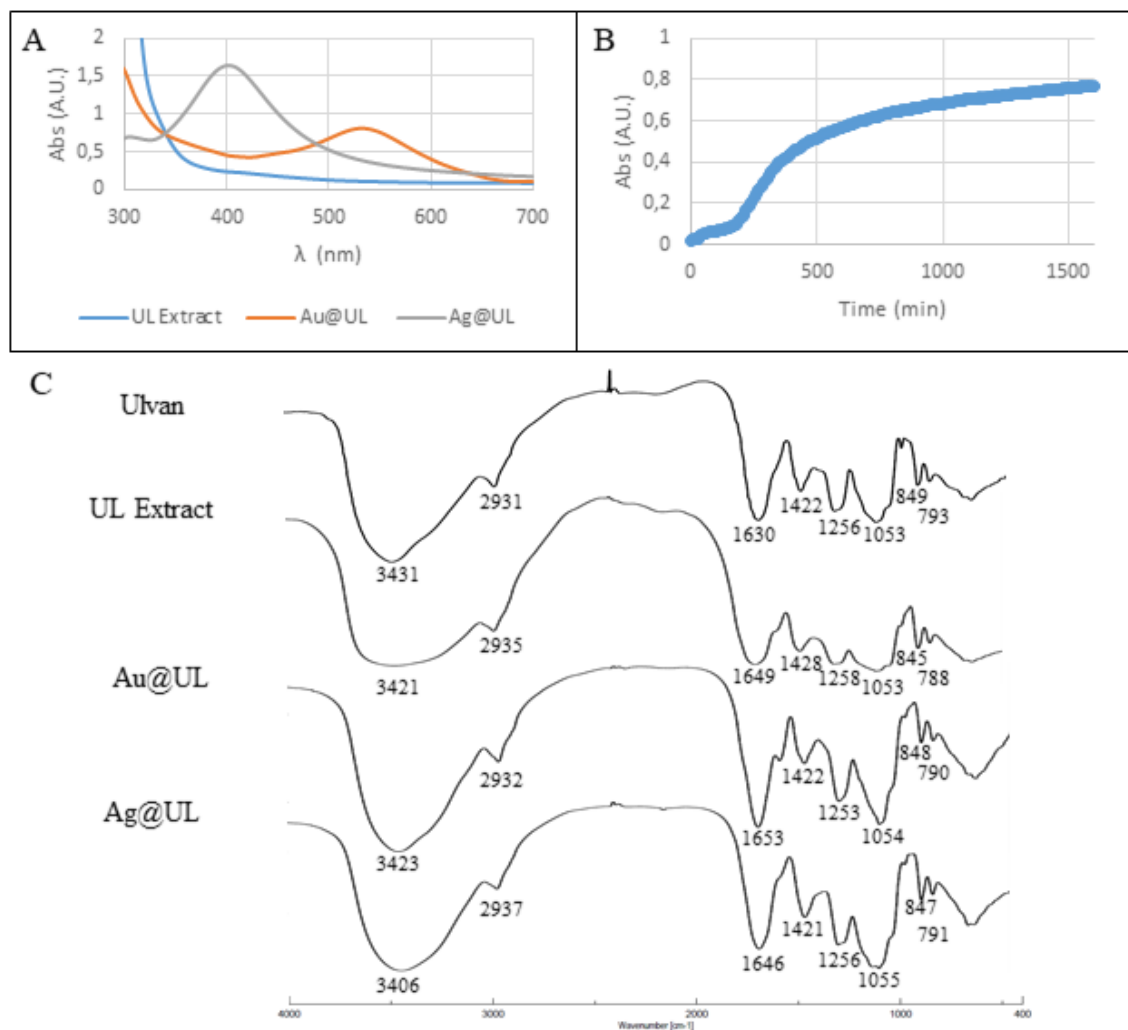
Figure 2. A) UV-Vis spectra of UL extract, Au@UL and Ag@UL. B) Reaction progress during the synthesis of Au@UL. C) FT-IR spectra of Ulvan, UL extract and biosynthesized nanoparticles.

3.4. *Fourier Transform Infra-Red spectroscopy*

Fourier Transform Infra-Red spectral analysis was carried out to identify the biomolecules present in UL extract, Au@UL and Ag@UL. The FTIR bands were assigned on the basis of previous reports. [3,10,22,23]. There are several studies in the literature on FTIR analysis of Ulvan extracted from different species; therefore, the FTIR spectra from commercial Ulvan was used in the comparative analysis with our compounds (Figure 2C). First, some shifts in the main bands of Ulvan and UL extract were observed. Ulvan is present in the cell wall of green algae in close association

with proteins and other biomolecules [22]; hence, the shifts observed in our extract, could be modifications linked to the presence of these molecules in association with Ulvan.

The strong broad band seen at near 3400 cm^{-1} was assigned to NH stretching vibrations and OH stretching vibrations of hydroxy group of sugar, resulting from intermolecular and intramolecular hydrogen bonding. The weak band at around 2930 cm^{-1} can be assigned to stretching vibration of aliphatic C-H groups.

Carboxylate groups show two broad bands: an asymmetrical stretching band at around 1650 cm^{-1} and a weaker symmetric stretching band at 1420 cm^{-1}. The spectral signals at 1250, 1056, 850 cm^{-1} were assigned to the stretching of -SO$_3$H and C-O-S groups. Finally, the minor band at 790 cm^{-1} was related to sugar cycles.

Unlike in the case of *C. baccata,* when comparing the spectra of the UL extract with those of the nanoparticles synthesized, it was not observed the major shifts previously reported[6], although some difference in the intensity and form of the bands and slight shifts were observed. This could be in accordance with the results obtained in the carbohydrate analysis section, where some difference in the sugar profile was observed.

3.5. *Electron Microscopy characterization*

TEM images were taken to characterize the size and shape of the obtained nanoparticles. The calculation of the size distribution histogram was based on the measurement of a significant number of nanoparticles (>100). In the case of gold, the mean diameter was 7.9 ± 1.7 nm (**Figure 3**A), while in the case of silver nanoparticles, larger sizes were obtained, with an average diameter of 31±8 nm (Figure 3B).
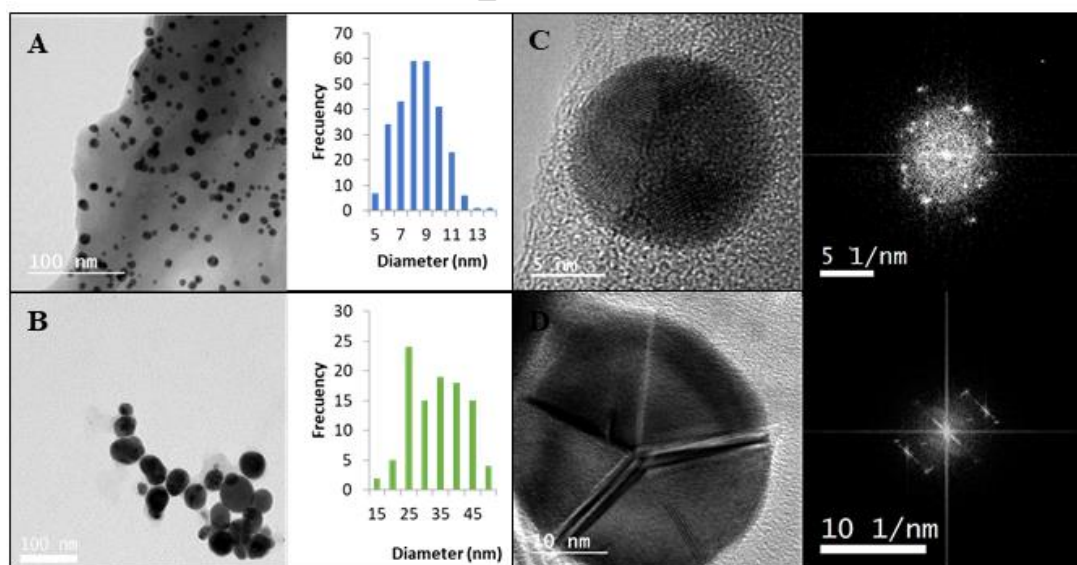
Figure 3. TEM images of Au@UL (A) and Ag@UL(B) with their corresponding size distribution histogram. HRTEM images of Au@UL (C) and Ag@UL (D) and their corresponding Fourier Transform.

To the best of our knowledge, this is the first report on the synthesis of gold nanoparticles led by *Ulva lactuca*, therefore we can only compare the size distribution with other seaweed extracts. Au@UL presented the lowest diameter related to other seaweeds tested by our group. The nanoparticles obtained under the same reaction conditions by the brown seaweed *Cystoseira baccata*,[6] have a diameter of 8.4 nm, whereas in the case of the Antaric seaweeds *Desmarestia menziesii* and *Palmaria decipiens,* a larger sizes were, with mean diameters of 11.5 and 36.8 nm respectively.[15] It is worth to highlight the small size obtained, since stable nanoparticles smaller than 10 nm diameter are difficult to synthesize.

Regarding the silver nanoparticles, previous studies on the synthesis of AgNP led by UL have reported on different size distributions that were linked to the reaction conditions. In most of the cases the nanoparticles presented a broad size distribution. Devi and Bhimba obtained a wide size distribution between 20 and 56 nm when using an autoclave at 121ºC for 10 min.[13] Valentin and Kumari obtained similar results with a size distribution between 20 and 50 nm, performing the synthesis at room temperature for 12 h.[10] On the other hand, Raja *et al.* obtained lower diameters (10-30 nm) heating at 70 ºC until the color changed.[20] Kumar *et al* and Sangeetha and Saravanan both performed the synthesis at room temperature during 48 and 72 h respectively[12,19]. They did not provide data about the size distribution, but only the mean diameters of 48.59 and 20 nm. However, in their TEM and SEM images, it can be observed the polydispersity of the samples. On the contrary, our study showed that we were able to optimaze the size distribution of our samples.

HRTEM images of Au@UL (Figure 3C) and Ag@UL (Figure 3D) provided information on the crystalline nature of the nanoparticles. In both cases the nanoparticles displayed internal complex contrast. Fourier Transform analysis confirmed that all the nanoparticles investigated were polycrystalline, having several crystalline domains. This can be clearly observed in the Ag@UL image (Figure 3D), where the irregularities of the particle surface can be noted. Some studies reveled that the polycrystallinity of nanoparticles increases the optical properties when compared with single-crystal nanoparticles.[24] Furthermore, the surface defects increase the number of reactive points, thus intensifying the reactivity of the nanoparticles.

DF-STEM images were also obtained (Figure 4A and B). In this kind of images, the contrast is related with the atomic number (Z) of the sample. In this sense, gold and silver appeared with a brighter contrast surrounded by a mass with darker contrast. The Energy Dispersive X-ray Analysis (Figure 5A and B) showed the presence of C, Cl, K, O, Mg, Na, S. In both cases, the elemental mapping (Figure 4C and D) confirmed C surrounding the metal nanoparticles. The other elements presented in the samples have been reported to be part of the biomolecules and minerals of UL.[25] In the EELS analysis we observed the characteristic edge of C, N and O, therefore confirming the

organic nature of the mass surrounding the nanoparticles (Figure 5C and D). Hence, the nanoparticles are enbebbed in the UL extract, which acts as a protective agent that keeps the particles separated, avoiding their aggregation.
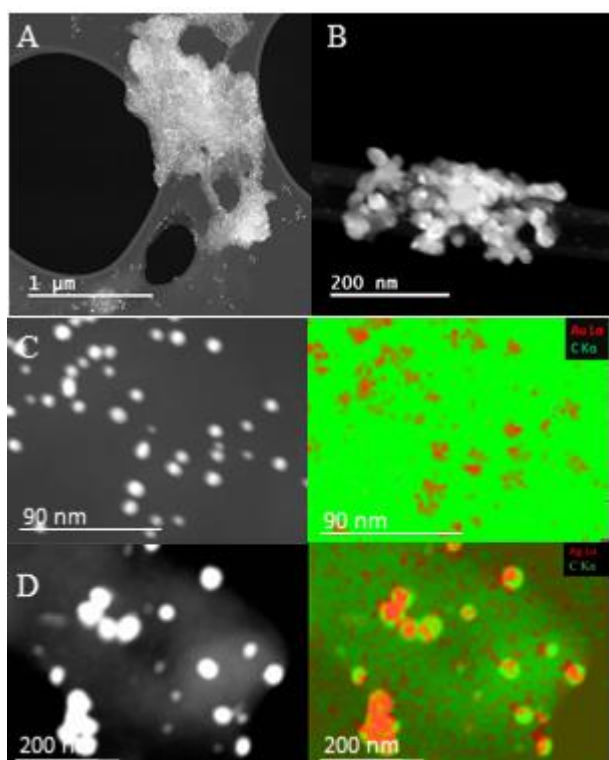
Figure 4. DF-STEM images showing Z-contrast of Au@UL (A) and Ag@UL (B) at different magnifications. STEM images of Au@UL (C) and Ag@UL (D), and their corresponding elemental mapping.
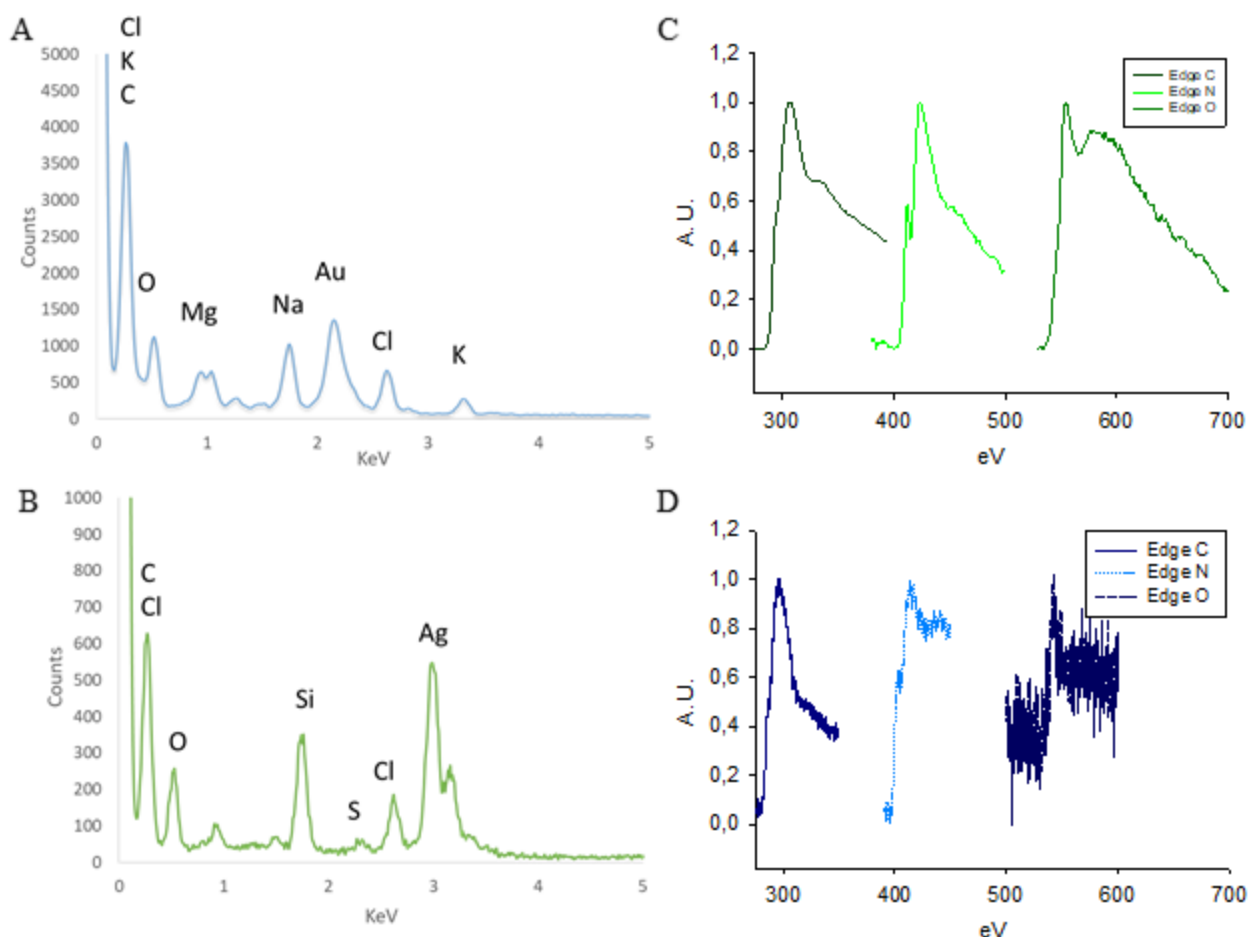
Figure 5. EDX analysis of Au@UL (A) and Ag@UL (B). EELS spectra of Au@UL (C) and Ag@UL (D).

3.6. *In vitro* antioxidant activity

Table 1 shows the reducing power, the total phenolic content and DPPH scavenging activity of *U. lactuca* extract prior and after the synthesis. These assays were performed in order to analyse UL extract potential to act as reducing agent in the synthesis of gold and silver nanoparticles. The reducing capacity of the extract was found to be appreciable, with a value of 24.3 ± 0.5 mg Ascorbic Acid/g seaweed. This confirmed the presence of reductants in the extract. In this case a comparison with literature data is a difficult task, due to the current lack of an official standard method to standarize reference substances used for the determination of the reducing activity. Nevertheless, we have compared our results with those previously obtained for the br own alga *Cystoseira baccata*.[6] It is remarkcable that the brown alga has 24 times more reducing activity than the green seaweed. Also, UL extract exhibit 5 times lower reducing power than the brown Antartic macroalgae *Desmarestia menziesii* and 2 times lower than the Rhodophyta *Palmaria decipiens*.[15] We are willing to study how this difference in reducing power affects the synthesis of nanoparticles.

Total phenolic compounds (TPC) present in the extract were also analyzed. It has been reported the direct correlation between TPC and antioxidant activity. The value obtained for UL extract was 0.13 ± 0.02 mg gallic acid equivalent (GAE)/g of seaweed. The low value obtained is in accordance with the literature. Boisvert *et al.* reported the TPC of an ethanolic extract of UL obtaining 6.9 ± 0.01 mg GAE/g.[26] The increase observed matched with studies that demonstrated that ethanolic extracts posses higher TPC than aqueous extracts [27]. When comparing this result with the one obtained for *C. baccata,* it was observed that UL extract had 18 times less phenolic content. In the same way, UL extract contains 6 and 3 times lower phenolic content than *D. menziesii* and *P. decipiens* respectively.

Finally, UL extract presents an EC50 value of 153.8 mg/mL. Results revealed that the extract contains free radical scavengers which reacted with DPPH radicals by their electron-donating ability. Reserchers in the literature reported different EC50 values for UL extracts. Boisvert *et al* reported an EC50 value of 58.9 µg/mL for an ethanolic extract.[26] Previous researchers noted an EC50 of 1266.7 µg/mL for UL with 96% ethanol.[28] These differences in the values obtained with aqueous or alcoholic extracts could be explained since the use of different solvents has been reported to interfere with the DPPH radical.[29] Variation in solvent polarity could modify the efficiency to retrieve a specific group of compounds, and therefore influences the antioxidant properties of the extracts.[28]

In the case of the nanoparticles, when compared with UL extract, the results obtained showed a decrease of 1.2 times in Au@UL reducing power, an increase of 1.8 times in the total phenolic content and a decrease in the EC50 value. Regarding Ag@UL, there was a 1.3 times increase in the reducing power, a 2.5 times increase in total phenolic content and a 3.3 times decrease in the EC50. These results well agree with other studies stating that, although the phytoconstituents of the seaweeds plays a major role in the antioxidant activity, the presence of nanoparticles enhances the values obtained.[30] In general, we observed higher antioxidant activity in Ag@UL compared with Au@UL, which could relate to the fact that silver acts as a good reducent and can lose electrons easier than gold.[17,31] Nevertheless, these results demonstrate that the biosynthesized nanoparticles showed promising prospectives for the development of novel antioxidant agents.

Table 1. Reducing activity, total phenolic content, and DPPH scavenging activity of *Ulva lactuca* extract, Au@UL and Ag@UL.

	Reducing activity (mg ascorbic acid/g seaweed)	Total phenolic content (mg galic acid/g seaweed)	DPPH scavenging activity (EC50 mg/mL)
UL extract	24.3±0.5	0.13±0.02	153.8
Au@UL	19.7±1.3	0.24±0.02	135.2
Ag@UL	31.6±1.5	0.32 ± 0.01	47.75

3.7. In vitro anticancer activity of Au@UL, Ag@UL and UL extract

The cytotoxic activity of the UL extract, Au@UL and Ag@UL was tested in the human colon cancer cell lines Caco-2 and HT-29. The normal cell lines PCS-201-010 and CCD-112CoN were used as control of the effect in healthy cells.

In this study, we have shown that UL extract did not induce cytoxicity in healthy cell lines, but it did it in the CRC cell lines at a dosage of 1g/mL with viabilities of 49.8±1.1% and 37.7±2.3% for Caco-2 and HT-29, respectively.
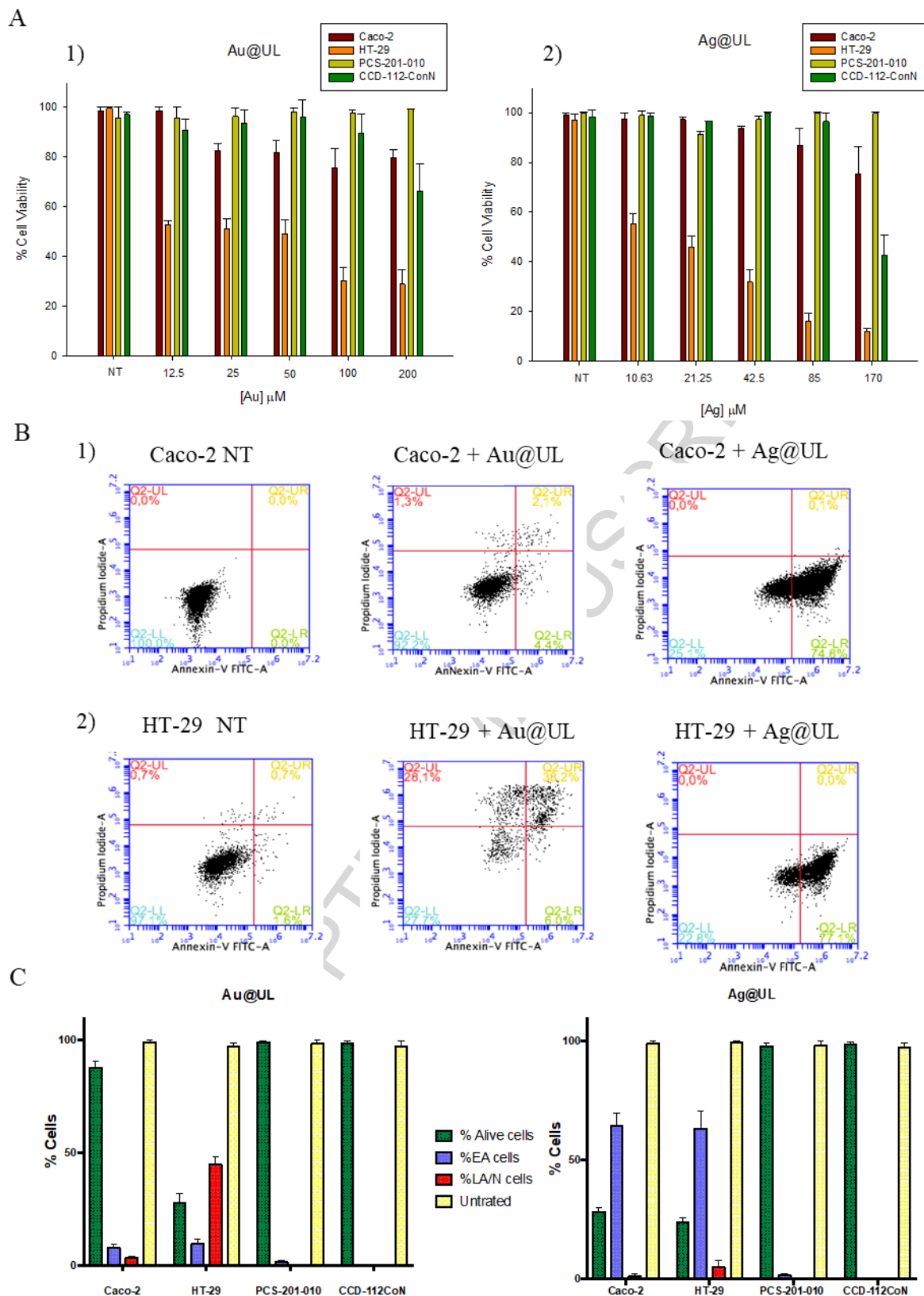
The dosage effect of Au@UL and Ag@UL on the cytotoxicity is shown in Figure 6A. No significant cytotoxic effect was observed in the healthy lines PCS-201-010. Meanwhile, in CCD-112CoN the only significant dosage effect was at 200 μM in the case of Au@UL and at 170 μM for Ag@UL. In terms of the CRC lines, the analyses revealed that the Au@UL and Ag@UL presented a pronounced effect in HT-29 at all the doses tested. The calculated IC50 values in HT-29 were 23μM for Au@UL and 13μM for Ag@UL.

Multiple studies explored the use of gold nanoparticles for cancer therapy.[14] Recent studies agree that AuNPs infiltrate into the tumoral tissue, where it accumulates into the extracellular matrix before entering the cells. RelevantTo improve the killing efficiency, studies are under development, addressed to accumulate nanoparticles in the sub-cellular compartments to destroy intrinsic cancer cell functions using the nucleus, mitochondria and the endoplasmic reticulum as targets.[32]

There are a number of studies showing the antiproliferative properties of silver nanoparticles, albeit there is gap in even if they do not explore the biological processes that induce this effect. On the contrary, a few studies report on the anticancer activity of silver nanoparticles[33]. In this regard, as previously mentioned, Devi and Bhimba[13], reported that activity of AgNPs is related with the aqueous extract of UL. These authors attain an IC50 value for HT-29 of 49 μg/mL. In contrast, the Ag@UL obtained in our study had an IC50 of 1.40 μg/mL when tested against the same cell line. Furthermore, other studies using silver compounds synthesized with other algae and plants extracts have shown a higher IC50 against HT-29 and other cancer cell lines.[30,34,35]

In Caco-2, both Au@UL and Ag@UL have percentages of viability close to 80%, even at the highest dosage used. As a result, they have a low cytotoxic effect. Several studies have raised the issue of cytotoxic activity in cancer models, leading to controversial results. For example, in Caco-2 cells it has been claimed that viability percentages of over 80% in cytotoxicity activity exist at dosages higher than those used in our study.[36,37] Recent results demonstrated that gold nanoparticles synthesized using *C. baccata* extract showed cytotoxic activity in Caco-2 with an IC50 of 79.03 μM.[6]

Figure 6. A) % Cell viability of 1) Au@UL and 2) Ag@UL for the four cell lines at different concentrations. B) Cytometry dot plots showing Annexin V-FITC and PI staining of Caco-2 and HT-29 (1) Untreated control Caco-2, Caco-2 exposed to Au@UL and Caco-2 exposed to Ag@UL. (2) Untreated control HT-29, HT-29 exposed to Au@UL and Ag@UL. C) Summary of the % of cells

under EA (early apoptosis) and LA/N (late apoptosis/necrosis) for Au@UL, Ag@UL and untreated cell lines Caco-2, HT-29, PCS-201-010 and CCD-112CoN.

Our results evidenced that the cytotoxic effect of Au@UL and Ag@UL was specific to the CRC cell lines and did not produce significant toxicities at IC50 doses on the healthy cells, therefore increasing the therapeutic interest of the new synthetized compounds.

3.8. Cell death induced by nanoparticles

The mechanism of cell death induced by Au@UL and Ag@UL were examined in HT-29 and in Caco-2, even if they didn't present a strong cytotoxic effect in this cell line. The normal fibroblastic line PCS-201-010 and the colon normal cell line CCD-112CoN were also included as controls. As criterion for apoptosis, the phospholipid phosphatidylserine (PS) redistribution from the inner to the outer leaflet of the plasma membrane lipid bilayer, and membrane permeabilization were tested by flow cytometry using Annexin V-FITC and propidium iodide (PI). Flow cytometry dot plots from one of the replicates are shown in Figure 6B.

A bar chart with the percentage of cells in early apoptosis and late apoptosis/necrosis build with all the replicates are shown in Figure 6C. The treatment of Au@UL induced a 12-fold rise in early apoptotic cells in Caco-2 when compared with the untreated control, while a 10 fold rise was detected for HT-29.

When comparing the % of cells in early apoptosis, it is similar in Caco-2 (7.8±3.3%) and in HT-29 (9.6±3.5%). However, the % of cells detected in late apoptosis/necrosis was significantly higher (13-fold) in HT-29 (44.7± 6.1%) than those in Caco-2 (3.3±1.4%). Moreover, the % of cells from HT-29 in late apoptosis/necrosis was 440-fold higher than those in the untreated control, and 33-fold higher in the case of Caco-2. No effect was detected when comparing untreated *vs.* treated PSC-201-010 and CCD-112CoN cultures. The treatment with Ag@UL resulted in a similar effect in terms of early apoptotic cells for both CRC cell lines. Meanwhile the % of cells detected in late apoptosis/necrosis was 50-fold higher in HT-29 than in Caco-2.

When the effect of both compounds in terms of early apoptosis induction was studied, the effect of Ag@UL was around 9-fold higher for both CRC cell lines when compared with the cells treated with Au@UL. The differences in late apoptosis necrosis stage were only remarkable in the cell line HT-29 treated with Au@UL. In the present study, the standart procedure to monitor the progression of apoptosis was used; however, it doesn't allow us to discriminate between late apoptotic and primary necrotic cells, since both these groups of cells are Annexin V-FITC$^+$/PI$^+$. To distinguish necrotic from late apoptotic cells, caspase assays and other flow cytometry assays with antibodies bind to intracellular apoptotic markers will be employed in future studies. [38]

3.9. Nanoparticle cellular uptake

Understanding the interaction of nanoparticles with the different type of cells is crucial to develop more effective nanoparticle based treatments. It has been reported that nanoparticles can enter the cell via a combination of different routes.[39] Silver and gold nanoparticles uptake has been studied by other authours before using microscopy techniques.[40,41] In the present study, we detected the cell internalization of Au@UL and Ag@UL by flow cytometry using a modification of the protocol proposed by Zuker.[16] Results showed that after 12 hours of incubation, the internalization was higher in the case of the Au@UL (Figure 7). It is remarkable that no internalization was detected for Ag@UL in the healthy cell line PSC-201-010. However, for Au@UL we got a positive signal. To the best of our knowledge, this is the first evidence of detection of gold nanoparticles internalization just by using cytometry and gold surface plasmon resonance (SPR) properties. Both gold and silver nanoparticles presented SPR, as evidenced by the detection of a signal in the far-red fluorescence spectral channel when the cell internalizes the nanoparticles. None signal was detected in the non-treated cells employed as control. Moreover, the internalization can be also detected by an increase in the Side-scattered (SSC). The SSC signal is proportional to the cell internal complexity and granularity. Our results showed that when cells are treated with Au@UL and Ag@UL there was an increase in the SSC signal (data not shown).

PE Texas-Red-A
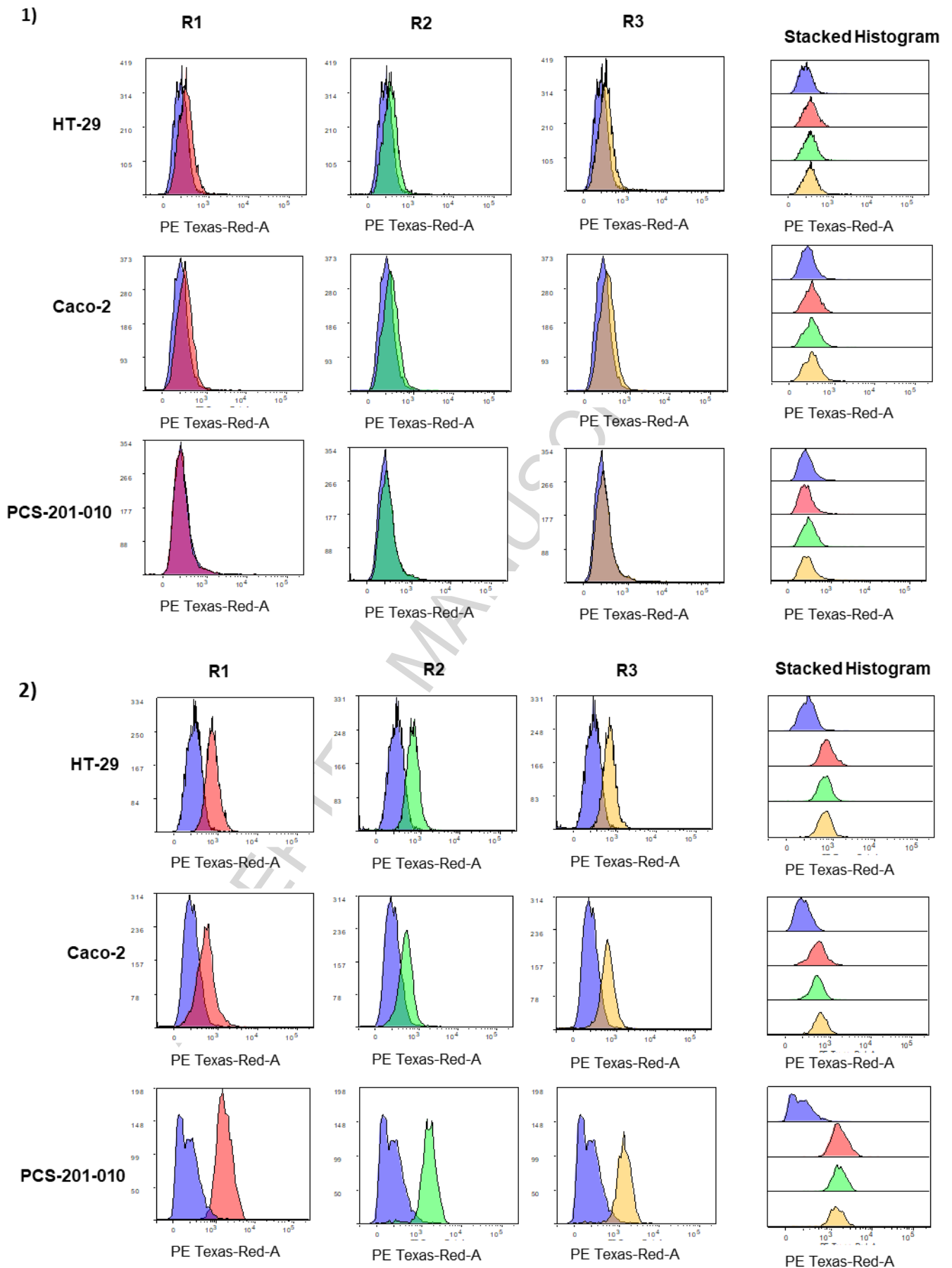
Figure 7. Histograms overlays for the Caco-2, HT-29 and PCS-201-010 after 12 hours culture with: 1) Ag@UL and 2) Au@UL. R1= replicate 1, R2= replicate 2, R3= replicate 3. Overlays of the three replicates (red, green and yellow) with the non-treated cells (blue). Stacked histograms with all the replicates and the non-treated cells were obtained with the Flowlogic software.

Factors such as geometry, size and surface morphology have a relevant influence on the nanoparticles cellular uptake.[42,43] Further, smaller nanoparticles can enter and exit the cell more efficiently.[44] This observation explains the high uptake of AuNPs by the CRC epithelial cells and the fibroblast cell line. The size of the AgNP was 31±8 nm, meanwhile the synthetized gold nanoparticles were four times smaller (7.9± 1.7nm). Moreover, phagocytic cells uptake anionic nanoparticles, whereas nonphagocytic cells favor cationic NPs internalization, with charge density and hydrophobicity being also important factors.[45] Several types of cells including epithelial cells and fibroblast can internalize nanoparticles by phagocytosis.[39] Both Caco-2 and HT-29 have phagocytic capacity.[46,47] Indeed, both nanoparticle compounds have negative charge: Au@UL -27.8 ± 0.6 mV and Ag@UL -16.0±0.4 mV. The highest negative charge of the gold nanoparticles together with size explain their higher uptake by the cell lines studied. It is reasonable to think that the higher uptake of Au@UL will result in a high cytotoxicity of the compound.

However, the higher cytotoxic effect is presented by Ag@UL. This apparent contradiction can be explained by the fact that charged gold nanoparticles are more cytotoxic than neutral or negative ones.[48] Despite Ag@UL presentedpresente a weak internalization, its action resulted to be stronger. Several works showed that silver nanoparticles are more toxic than gold nanoparticles in different *in vitro* and *in vivo* models.[49,50] With regards to the uptaking process, a recent study [51] showed that Ag NP uptake by macrophages can be affected by their size and by the presence or absence of serum proteins in the media, with fetal calf serum presenting a higher silver nanoparticles uptake.

4. Conclusions

We have described an efficient method for the biosynthesis of gold and silver nanoparticles using *Ulva lactuca* aqueous extract. A full characterization using UV-Vis spectroscopy, TEM, HRTEM, STEM, Z Potential and FTIR spectroscopy was performed. For the first time in scientific literature, the composition of carbohydrates of UL extract and the changes observed after nanoparticles synthesis were studied, in order to investigate their possible role in the biosynthetic process. The reducing power, total phenolic content and DPPH scavenging activity of UL extract, Au@UL and Ag@UL were determined.

Both Au@UL and Ag@UL were tested against two colorectal cancer cell lines (HT-29 and Caco-2), presenting the highest cytotoxic activity in HT-29 with Ag@UL, with an IC50 of 13 μM.

Our results showed that both Au@UL and Ag@UL are able to induce apoptosis in the CRC cell lines. The rate of internalization for Au@UL is higher than that for Ag@UL. This is the first evidence of detection of gold nanoparticles internalization just by using cytometry.

Both Au@UL and Ag@UL exhibit excellent biocompatibility on the healthy cell lines PCS-201-010 and CCD-112CoN at regular doses. Overall, our results suggest that Au@UL and Ag@UL have a significant potential for the treatment of colorectal cancer. Consequently, further studies should be addressed to explore the internalization routes and the biochemical mechanisms underlying the Au@UL and Ag@UL apoptotic capacities.

References

[1] T. Khan, P. Gurav, PhytoNanotechnology: Enhancing Delivery of Plant Based Anti-cancer Drugs, Front Pharmacol. 8 (2017) 1002.

[2] P. Manivasagan, J. Oh, Marine polysaccharide-based nanomaterials as a novel source of nanobiotechnological applications, Int J Biol Macromol. 82 (2016) 315-327.

[3] H. Tian, X. Yin, Q. Zeng, L. Zhu, J. Chen, Isolation, structure, and surfactant properties of polysaccharides from *Ulva lactuca* L. from South China Sea, Int. J. Biol. Macromol. 79 (2015) 577-582.

[4] S.A. Dahoumane, M. Mechouet, K. Wijesekera, C.D.M. Filipe, C. Sicard, D.A. Bazylinski, C. Jeffryes, Algae-mediated biosynthesis of inorganic nanomaterials as a promising route in nanobiotechnology – a review, Green Chemistry. 19 (2017) 552-587.

[5] K. Ponnuchamy, J.A. Jacob, Metal nanoparticles from marine seaweeds-a review, Nanotechnology Reviews. 5 (2016) 589-600.

[6] N. González-Ballesteros, S. Prado-López, J.B. Rodríguez-González, M. Lastra-Valdor, M.C. Rodríguez-Argüelles, Green synthesis of gold nanoparticles using brown seaweed *Cystoseira baccata:* Its activity in colon cancer cells, Colloids Surf. B. Biointerfaces. 153 (2017) 190-198.

[7] J. Venkatesan, B. Lowe, S. Anil, P. Manivasagan, A.A. Al-Kheraif, K.H. Kang, S.K. Kim, Seaweed polysaccharides and their potential biomedical applications, Starch/Staerke. 67 (2015) 381-390.

[8] G.E.F. Abd-Ellatef, O. Ahmed, E.S. Abdel-Reheim, A. Abdel-Hamid, Ulva lactuca polysaccharides prevent Wistar rat breast carcinogenesis through the augmentation of apoptosis, enhancement of antioxidant defense system, and suppression of inflammation, Breast Cancer: Target and Therapy. 9 (2017) 67-83.

[9] O.M. Ahmed, R.R. Ahmed, Anti-proliferative and apoptotic efficacies of ulvan polysaccharides against different types of carcinoma cells in vitro and in vivo, Journal of Cancer Science and Therapy. 6 (2014) 202-208.

[10] B.B. Valentin, P.R. Kumari, Phytosynthesis of silver nanoparticles from the extracts of seaweed *Ulva lactuca* and its antimicrobial activity, Int J Pharm Bio Sci. 5 (2014) 666-677.

[11] K. Murugan, C.M. Samidoss, C. Panneerselvam, A. Higuchi, M. Roni, U. Suresh, B. Chandramohan, J. Subramaniam, P. Madhiyazhagan, D. Dinesh, R. Rajaganesh, A.A. Alarfaj, M. Nicoletti, S. Kumar, H. Wei, A. Canale, H. Mehlhorn, G. Benelli, Seaweed-synthesized silver nanoparticles: an eco-friendly tool in the fight against Plasmodium falciparum and its vector Anopheles stephensi? Parasitol. Res. 114 (2015) 4087-4097.

[12] P. Kumar, M. Govindaraju, S. Senthamilselvi, K. Premkumar, Photocatalytic degradation of methyl orange dye using silver (Ag) nanoparticles synthesized from *Ulva lactuca*, Colloids and surfaces. B, Biointerfaces. 103 (2013) 658-661.

[13] J.S. Devi, B.V. Bhimba, Anticancer Activity of Silver Nanoparticles Synthesized by the Seaweed *Ulva lactuca In vitro*, Open Acces Scientific Report. 02 (2012) 1-5.

[14] N. Elahi, M. Kamali, M.H. Baghersad, Recent biomedical applications of gold nanoparticles: A review, Talanta. 184 (2018) 537-556.

[15] N. González-Ballesteros, J.B. Rodríguez-González, M. Lastra-Valdor, M.C. Rodriguez Argüelles, New application of two Antarctic macroalgae *Palmaria decipiens* and *Desmarestia menziesii* in the synthesis of gold and silver nanoparticles, Polar Science. 15 (2018) 49-54.

[16] R.M. Zucker, K.M. Daniel, E.J. Massaro, S.J. Karafas, L.L. Degn, W.K. Boyes, Detection of Silver Nanoparticles in Cells by Flow Cytometry Using Light Scatter and Far-Red Fluorescence, Citometry Part A. 83 (2013) 962-972.

[17] D. Wang, J. Markus, C. Wang, Y.J. Kim, R. Mathiyalagan, V. Aceituno-Castro, S. Ahn, D.C. Yang, Green synthesis of gold and silver nanoparticles using aqueous extract of *Cibotium barometz* root, Artificial cells, nanomedicine and biotechnology. 45 (2017) 1548-1555.

[18] K. Anuradha, P. Bangal, S.S. Madhavendra, Macromolecular arabinogalactan polysaccharide mediated synthesis of silver nanoparticles, characterization and evaluation, Macromolecular Research. 24 (2016) 152-162.

[19] N. Sangeetha, K. Saravanan, Biogenic Silver Nanoparticles using Marine Seaweed (*Ulva lactuca*) and Evaluation of its Antibacterial activity, Journal of Nanoscience and Nanotechnology. 2 (2014) 99-102.

[20] S.B. Raja, J. Suriya, V. Sekar, R. Rajasekaran, Biomimetic of silver nanoparticles by *Ulva lactuca* seaweed and evaluation of its antibacterial activity, International Journal of Pharmacy and Pharmaceutical Sciences. 4 (2012) 139-143.

[21] C. Tiloke, A. Phulukdaree, K. Anand, R.M. Gengan, A.A. Chuturgoon, Moringa oleifera Gold Nanoparticles Modulate Oncogenes, Tumor Suppressor Genes, and Caspase-9 Splice Variants in A549 Cells, Journal of Cellular Biochemistry. 9999 (2016) 1-13.

[22] A. Alves, R.A. Sousa, R.L. Reis, In vitro cytotoxicity assessment of ulvan, a polysaccharide extracted from green algae, Phytotherapy Research. 27 (2013) 1143-1148.

[23] G. El-Said, M. El-Sadaawy, M. Aly-Eldeen, Adsorption isotherms and kinetic studies for the defluoridation from aqueous solution using eco-friendly raw marine green algae, Ulva lactuca, Environ. Monit. Assess. 190 (2018) 14-29.

[24] N. Goubet, I. Tempra, J. Yang, G. Soavi, D. Polli, G. Cerullo, M.P. Pileni, Size and nanocrystallinity controlled gold nanocrystals: synthesis, electronic and mechanical properties, Nanoscale. 7 (2015) 3237-3246.

[25] J. Debbarma, B. Madhusudana-Rao, L. Narasimha-Murthy, S. Mathew, G. Venkateshwarlu, C.N. Ravishankar, Nutritional profiling of the edible seaweeds *Gracilaria edulis*, *Ulva lactuca* and *Sargassum sp*. Indian Journal of Fisheries. 63 (2016) 81-87.

[26] C. Boisvert, L. Beaulieu, C. Bonnet, E. Pelletier, Assessment of the antioxidant and antibacterial activities of three species of edible seaweeds, J Food Biochem. 39 (2015) 377-387.

[27] S.H. Cho, S.E. Kang, J.Y. Cho, A.R. Kim, S.M. Park, Y.K. Hong, D.H. Ahn, The Antioxidant Properties of Brown Seaweed (*Sargassum siliquastrum*) Extracts, Journal of medicinal food. 10 (2007) 479-485.

[28] K.H.S. Farvin, C. Jacobsen, Phenolic compounds and antioxidant activities of selected species of seaweeds from Danish coast, Food Chemistry. 138 (2013) 1670-1681.

[29] J. Pérez-Jiménez, F. Saura-Calixto, Effect of solvent and certain food constituents on different antioxidant capacity assays, Food Research International. 39 (2006) 791-800.

[30] S. Palanisamy, P. Rajasekar, G. Vijayaprasath, G. Ravi, R. Manikandan, N.M. Prabhu, A green route to synthesis silver nanoparticles using *Sargassum polycystum* and its antioxidant and cytotoxic effects: An in vitro analysis, Mater Lett. 189 (2017) 196-200.

[31] V. Soshnikova, Y.J. Kim, P. Singh, Y. Huo, J. Markus, S. Ahn, V. Castro-Aceituno, J. Kang, M. Chokkalingam, R. Mathiyalagan, D.C. Yang, Cardamom fruits as a green resource for facile synthesis

of gold and silver nanoparticles and their biological applications, Artificial cells, nanomedicine and biotechnology. 46 (2018) 108-117.

[32] H. Sun, J. Jia, C. Jiang, S. Zhai, Gold Nanoparticle-Induced Cell Death and Potential Applications in Nanomedicine, International Journal of Molecular Sciences. 19 (2018) 754.

[33] S.U. Khan, A. Saleh, A. Wahab, M.H.U. Khan, D. Khan, W.U. khan, A. Rahim, S. kamal, F.U. khan, S. Fahad, Nanosilver: new ageless and versatile biomedical therapeutic scaffold, International Journal of Nanomedicine. 13 (2018) 733-762.

[34] M. Sengani, D. Rajeswari, Cytotoxicity and apoptotic effect of biogenic silver nanoparticles on human colorectal cell line HT-29, Research Journal of Biotechnology. 11 (2016) 65-70.

[35] B. Srinithya, V.V. Kumar, V. Vadivel, B. Pemaiah, S.P. Anthony, M.S. Muthuraman, Synthesis of biofunctionalized AgNPs using medicinally important *Sida cordifolia* leaf extract for enhanced antioxidant and anticancer activities, Mater Lett. 170 (2016) 101-104.

[36] E. Bajak, M. Fabbri, J. Ponti, S. Gioria, I. Ojea-Jiménez, A. Collotta, V. Mariani, D. Gilliland, F. Rossi, L. Gribaldo, Changes in Caco-2 cells transcriptome profiles upon exposure to gold nanoparticles, Toxicol Lett. 233 (2015) 187-99.

[37] A.F. Martins, S.P. Facchi, J.P. Monteiro, S.R. Nocchi, C.T.P. Silva, C.V. Nakamura, E.M. Girotto, A.F. Rubira, E.C. Muniz, Preparation and cytotoxicity of N,N,N-trimethyl chitosan/alginate beads containing gold nanoparticles, Int. J. Biol. Macromol. 72 (2015) 466-471.

[38] E. Brauchle, S. Thude, S.Y. Brucker, K. Chenke-Layland, Cell death stages in single apoptotic and necrotic cells monitored by Raman microspectroscopy, Scientific Reports. 4 (2014) 4698.

[39] B. Yameen, W.I. Choi, C. Vilos, A. Swami, J. Shi, O.C. Farokhzad, Insight into nanoparticle cellular uptake and intracellular targeting, J. Controlled Release. 190 (2014) 485-499.

[40] M. van der Zande, A.K. Undas, E. Kramer, M.P. Monopoli, R.J. Peters, D. Garry, E.C. Antunes Fernandes, P.J. Hendriksen, H.J.P. Marvin, A.A. Peijnenburg, H. Bouwmeester, Different responses of Caco-2 and MCF-7 cells to silver nanoparticles are based on highly similar mechanisms of action, Nanotoxicology. 10 (2016) 1431-1441.

[41] F. Moser, G. Hildenbrand, P. Müller, A. Al Saroori, A. Biswas, M. Bach, F. Wenz, C. Cremer, N. Burger, Marlon R., M.l. Hausmann, Cellular Uptake of Gold Nanoparticles and Their Behavior as Labels for Localization Microscopy, Biophys J. 110 (2016) 947-953.

[42] R.S. Petros, J.M. DeSimone, Strategies in the design of nanoparticles for therapeutic applications, Nature Reviews Drug Discovery. 9 (2010) 615-627.

[43] N. Bertrand, J. Wu, X. Xu, N. Kamaly, O.C. Farokhzad, Cancer nanotechnology: The impact of passive and active targeting in the era of modern cancer biology, Adv. Drug Deliv. Rev. 66 (2014) 2-25.

[44] O. Nuri, J.O. Park, Endocytosis and exocytosis of nanoparticles in mammalian cells. Int J Nanomedicine. 9 (2014) 51-63.

[45] E. Fröhlich, The role of surface charge in cellular uptake and cytotoxicity of medical nanoparticles, International Journal of Nanomedicine. 7 (2012) 5577-5591.

[46] G.J. Leitch, T.L. Ward, A.P. Shaw, G. Newman, Apical spore phagocytosis is not a significant route of infection of differentiated enterocytes by Encephalitozoon intestinalis, Infect. Immun. 73 (2005) 7697-7704.

[47] J. Kopecka, I. Campia, D. Brusa, S. Doublier, L. Matera, D. Ghigo, A. Bosia, C. Riganti, Nitric oxide and P-glycoprotein modulate the phagocytosis of colon cancer cells, J. Cell. Mol. Med. 15 (2011) 1492-1504.

[48] N.M. Schaeublin, L.K. Braydich-Stolle, A.M. Schrand, Surface charge of gold nanoparticles mediates mechanism of toxicity, Nanoscale. 3 (2011) 410-420.

[49] P.V. Asharani, Y. Lianwu, Z. Gong, S. Valiyaveettil, Comparison of the toxicity of silver, gold and platinum nanoparticles in developing zebrafish embryos, Nanotoxicology. 5 (2011) 43-54.

[50] Z.E. Jiménez-Pérez, R. Mathiyalagan, J. Markus, Y.J. Kim, H.M. Kang, R. Abbai, K.H. Seo, D. Wang, V. Soshnikova, D.C. Yang, Ginseng-berry-mediated gold and silver nanoparticle synthesis and evaluation of their in vitro antioxidant, antimicrobial, and cytotoxicity effects on human dermal fibroblast and murine melanoma skin cell lines, J Nanomedicine. 12 (2017) 709-723.

[51] K. Kettler, C. Giannakou, W.H. de Jong, A.J. Hendriks, P. Krystek, Uptake of silver nanoparticles by monocytic THP-1 cells depends on particle size and presence of serum proteins, Journal of Nanoparticle Research. 18 (2016) 1-9.

Highlights

- Aqueous extract of *Ulva lactuca* served to synthesize gold and silver nanoparticles

- The composition of the extract before and after the synthesis was determined

- This provided new information about the possible role of sugars during the synthesis

- The effects of UL extract, Au@UL and Ag@UL were tested *in vitro* on colon cancer cells

- Apoptotic activity and cellular uptake evaluation was determined for Au@UL and Ag@UL